Available online at www.sciencedirect.com
SCIENCE DIRECT®
Coordination Chemistry Reviews 249 (2005) 197–208
COORDINATION CHEMISTRY REVIEWS
www.elsevier.com/locate/ccr

Review

Atomic resolution crystallography and XAFS

Richard W. Strange*, Mark Ellis, S. Samar Hasnain

CCLRC Daresbury Laboratory, Molecular Biophysics Group and North West Structural Genomics Centre, Warrington, Cheshire WA4 4AD, UK

Received 1 October 2003; accepted 12 March 2004
Available online 6 August 2004

Contents

Abstract

This review discusses the relationship between protein crystallography and X-ray absorption spectroscopy when applied to metalloproteins. The complementary nature of these two structural techniques is highlighted using recent examples. The importance of obtaining atomic resolution protein crystal data and the use of cryo-annealing are made clear, and the advantages of using the atomic resolution data in combination with X-ray absorption data are emphasised.

Keywords: EXAFS; Protein crystallography; Atomic resolution; Annealing; Metalloproteins

1. Introduction

Since the discovery of X-rays 100 years ago (Röntgen, 1895) the three-dimensional visualisation of matter has become possible at a level where the detailed architecture of even complex biological molecules can be understood. The pioneering work of Perutz and Kendrew in the 1940s and 1950s set the foundation of protein crystallography (PX) as a scientific activity whose success can only be described as phenomenal in the last thirty years. There are several reasons for this success but the availability of intense X-ray beams from synchrotron radiation (SR) sources, combined with powerful computers, has provided the major boost to this technique. The intense X-rays from SR have also been responsible for reviving another 'old' X-ray technique first discussed in the 1920s—X-ray absorption fine structure[1] (XAFS). Unlike crystallography, this technique is able to probe metal-containing proteins in both the aqueous and crystalline states, even though the majority of applications have been to the aqueous proteins. The technique provides sub-atomic resolution (∼0.2 Å) information centred about the metal centre in a metalloprotein. This information is localised to within a ∼5 Å sphere due to the short mean free path of the X-ray generated photoelectron whose scattering gives rise to the XAFS data. The full power of the technique is achieved when it is combined with three-dimensional structural data. This is usually available only from PX, which provides the structural data at variable resolution, ranging

* Corresponding author. Tel.: +44-1925-60-3273; fax: +44-1925-60-3748.
E-mail address: s.hasnain@dl.ac.uk (R.W. Strange).
URLs: http://www.srs.dl.ac.uk/mbg/, http://www.nwsgc.ac.uk/.

[1] The term XAFS refers to the X-ray absorption process as a whole and is normally divided into two regions: extended X-ray absorption fine structure (EXAFS) and X-ray absorption near edge structure (XANES). The EXAFS region provides the main information about distances, atom types and coordination numbers, while XANES is sensitive to metal oxidation state and coordination geometry.

0010-8545/$ – see front matter © 2004 Elsevier B.V. All rights reserved.
doi:10.1016/j.ccr.2004.03.019

Table 1
3D-EXAFS Cu–ligand distances [3] using Engh and Huber restraints [37] compared with 1.75 Å crystal structure values for oxidised and reduced *A. xylosoxidans* azurin II [2]

Ligand	Oxidised protein			Reduced protein		
	Crystallographic distance (Å)	EXAFS		Crystallographic distance (Å)	EXAFS	
		Distance (Å)	$2\sigma^2$ (Å^2)		Distance (Å)	$2\sigma^2$ (Å^2)
His117	1.99	1.94 (0.02)	0.002	2.02	2.01 (0.02)	0.002
His46	2.04	1.86 (0.02)	0.002	2.03	1.91 (0.02)	0.002
Cys112	2.14	2.12 (0.02)	0.001	2.16	2.19 (0.02)	0.001
Gly45	2.72	2.82 (0.05)	0.012	2.75	2.98 (0.05)	0.021
Met121	3.26	3.39	0.055	3.26	3.35	0.058
E_f (eV)	−9.27	0.61		−2.82	0.09	

The $2\sigma^2$ are the Debye–Waller terms.

from several Angströms to ∼1 Å. The usefulness of this combined approach for structure-function studies of metalloproteins will be demonstrated through several examples.

2. Why metalloproteins?

Metalloproteins form a large fraction (possibly up to 50%) of all known proteins. These contain metal ions either as single atom or as part of a cluster and play a variety of life sustaining roles in the bacterial, plant and animal kingdoms. In the list of 25 elements which have been recognised as essential and indispensable to life, 15 are metals. At least five of them (Na, K, Mg, Ca and Fe) appear to be crucial to every known form of life, whereas the other metals (V, Cr, Mn, Co Ni, Cu, Zn, Mo, W and Se) are required by some organisms. Some of the fundamental biological processes in which metalloproteins participate include electron storage and transfer, dioxygen binding, storage and activation, and substrate transport, catalysis and activation. Metalloproteins are known to be involved in several disease states and ageing processes. The incorporation of a metal ion in a protein in vivo is a very tightly regulated process that is often carried out by specific chaperon proteins. Failure to achieve this correctly can lead to the mis-function of these proteins leading to disease, and in general disease may arise from a variety of genetic factors. The mis-functions due to genetic alterations that lead to diseases like ALS (amyotrophic lateral sclerosis or motor neuron disease) and Creutzfeld Jacob disease (CJD) are now well recognised and involve metalloproteins.

3. XAFS and crystallographic resolution

In metalloproteins, the chemical and physical properties of metals are used to perform varied biological functions with great specification and control. To fully understand biological function it is essential to know not only the overall three-dimensional structure of these proteins but also the structure at the metal site to a resolution commensurate with the chemistry of a particular metal. It is therefore important to obtain very high resolution information about the metal centre with high precision (<0.05 Å) because the substrate-induced or redox-induced structural changes are generally very small (∼0.1 Å).

These changes are well within the error limits of most crystallographic determinations, since relatively few protein structures have been elucidated to atomic resolution. On the other hand, with XAFS the metal site can be probed with an accuracy and precision often approaching that routinely achieved in "*small molecule*" crystallography, while data can be collected on both aqueous and crystalline proteins with the *same resolution*.

These factors can be illustrated by the example of the structural changes that occur at the Cu centre of the electron transfer protein azurin during its oxidation–reduction cycle. The coordination of the Cu in this class of type 1 copper protein consists of two histidines, two sulphur donors (a cysteine and a methionine) and a peptide oxygen from glycine, arranged in a distorted trigonal bipyramid. Previously published crystallographic results at 1.8–1.75 Å resolution for oxidised and reduced azurin from *Alcaligenes denitrificans* [1] and *Alcaligenes xylosoxidans* [2] have suggested that no significant changes of the Cu site occur upon reduction. However, solution EXAFS data on azurin from *A. xylosoxidans* show statistically significant changes in Cu–ligand distances upon oxidation–reduction from 0.05 to 0.16 Å [3] (Table 1). A re-examination of the 1.75 Å crystallographic data in the light of the EXAFS result shows that changes in the Cu–S(cysteine) bond length upon oxidation or reduction of the metal are clearly evident in the crystallographic structures, but that the distances of the lighter N(His) atoms are not as accurately determined at such resolution due to Fourier ripple effect.

One advantage of SR based PX is that it has led to an increasing number of higher and higher resolution structures being determined (e.g. [4–6]) and several are now known at atomic resolution[2]. However, of some 250 structures of Cu

[2] Defined as the resolution at which individual atoms become clearly resolved, typically 1.2 Å [7]. At this resolution peptide carbons become resolved. High resolution is generally accepted to be <1.5 Å.

Table 2
Distribution of copper protein structures in the PDB, classified according to crystallographic resolution

Resolution of Cu–protein structures in the PDB

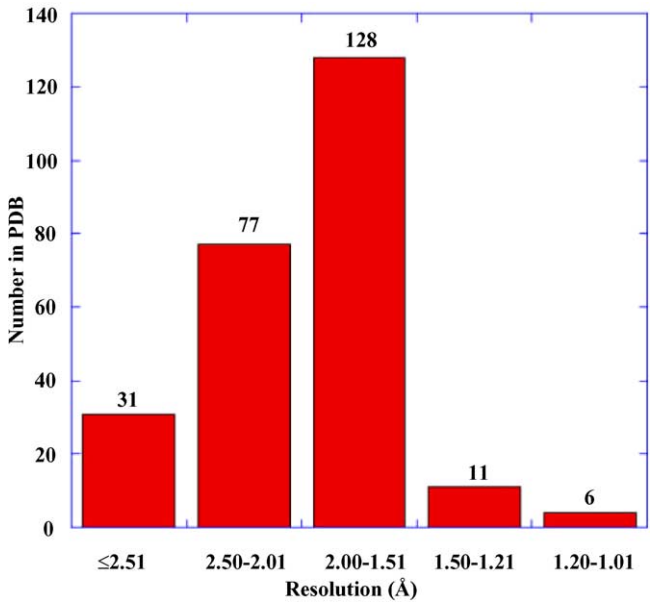

In more than 90% of structures the resolution is lower than 1.5 Å, with <2% reported at better than 1.2 Å resolution.

proteins in the Protein Data Bank (PDB [8]) only six are now known at atomic resolution, most of these appearing during the last 12 months. The same situation exists for metalloproteins containing other metals. The largest of the Cu-containing proteins for which atomic resolution data has been reported is the 1.09 Å resolution structure [9] of carbon monoxide dehydrogenase from *Oligotropha carboxydovorans* which contains a unique Cu–S–Mo catalytic centre that has also been characterised by XAFS [10]. The recent atomic resolution structure for *Achromobacter vinellandii* MoFe nitrogenase at 1.16 Å [11] has not only provided the increased accuracy of the structure but has revealed new features of fundamental biological importance. Thus, a nitrogen atom has been identified in the middle of six Fe atoms of the catalytically essential FeMo-cofactor. In previous crystal structures this central atom was not observed as it was masked by the Fourier ripples of the surrounding heavier Fe and S atoms. The electron density of this single N atom does not emerge until the resolution is extended beyond 1.55 Å. This 'Fourier ripple effect' from the heavy metal atoms in metalloproteins tends to undermine the accuracy of the metal–ligand bond distances observed in the crystal structures.

This is further illustrated by the example of the type 1 copper proteins (MW ∼ 12 kDa), where a number of high resolution crystal structures have become available (Table 2). Table 3 shows Cu–ligand distances determined by PX for the oxidised forms of plastocyanin from *Poplar nigra* [12], amicyanins from *Paraccocus denitrificans* [13,14] and *Thiobacillus versutus* [15] and azurins from *Pseudomonas aeruginosa* [16] and *Alcaligenes denitrificans* [17]. The resolution range for these structures varies from 1.9 Å to close to atomic, namely 1.31 Å for *P. denitrificans* amicyanin and 1.33 Å for plastocyanin. Also shown are the results of XAFS studies on oxidised spinach plastocyanin [18], amicyanin from *T. versutus* [19] and azurin from *P. aeruginosa* [20]. There are two important observations about these data. First, Guss et al. [12] noted that a shortening of the Cu–ligand distances for plastocyanin occurred as the crystal structure resolution improves from 1.6 to 1.33 Å. It is likely that this systematic shortening of the PX bond lengths versus resolution is due to a lessening of the Fourier ripple effect as the resolution of the structure improves. Second, a consistent feature of the XAFS results is that the Cu–ligand bond lengths are generally shorter than those found in the crystal structures. This is especially true of the Cu–N(histidine) bonds, which have always been found shorter by ∼0.1–0.2 Å, whereas there is better agreement (within ±0.03 Å) between PX structures (at any resolution) and solution XAFS when comparing the Cu–S(cysteine) distances. For both amicyanin and plastocyanin the agreement between PX and solution XAFS bond lengths improves as the crystal structure resolution increases and the errors associated with the PX bond lengths due to heavy atom Fourier ripple decrease.

The PX resolution limit for a metalloprotein is, therefore, critical, aside from the usual reasons, because of heavy atom Fourier ripple: if the resolution is too low it can obscure the presence of metal site ligands with low atomic number

Table 3
Cu–ligand bond lengths compared for several type 1 copper proteins, determined by PX and frozen solution XAFS studies

Resolution (Å)	Crystallographic Cu–ligand bonds (Å)					XAFS Cu–ligand bonds (Å)		
	Az_Pa 1.90	Az_Ad 1.80	Pl_Pn 1.6/1.33	Am_Pd 2.0/1.31	Am_Tv 2.15	Az_Pa pH 8.0	Pl_Sp pH 5.5	Am_Tv pH 5.2
Cu–N(His)	2.03	2.00	2.04/1.91	1.95/1.89	2.04	1.92	1.94	1.86
Cu–N(His)	2.11	2.08	2.10/2.06	2.00/1.97	2.13	1.92	2.02	1.95
Cu–S(Cys)	2.25	2.14	2.13/2.07	2.15/2.09	2.13	2.12	2.09	2.13
Cu–S(Met)	3.15	3.11	2.90/2.82	2.89/2.92	2.84	3.05	–	–
Reference	[16]	[17]	[12]	[13,14]	[15]	[20]	[18]	[19]

The proteins listed are: Az_Pa: *Pseudomonas aeruginosa* azurin; Az_Ad: *Alcaligenes denitrificans* azurin; Pl_Pn: *Poplar nigra* plastocyanin; Am_Pd: *Paracoccus denitrifcans* amicyanin; Am_Tv: *Thiobacillus versutus* amicyanin; Pl_Sp: Spinach plastocyanin.

or lead to inaccurate metal–ligand bond lengths. What may be considered "too low" in resolution is not easy to predict but practically speaking, if the objective is to get a detailed understanding of the metal environment one should make every effort to obtain atomic resolution structures.

4. Benefits of atomic resolution crystallography

The main advantages of atomic resolution crystallography are well understood [21] and the fact that only a small number of atomic resolution structures of metalloproteins are currently available is due a variety of factors, including the inherent diffraction limit due to crystalline disorder. Improving the diffraction limit by annealing [22–24], as in several of our own cases (Cu nitrite reductase, rusticyanin and bovine Cu–Zn superoxide dismutase), has significant promise. In the case of four copper proteins on which we have worked recently, the resolution is significantly improved after an in situ cryo-annealing procedure [24] compared to the first image taken at room temperature (or even following the initial exposure under cryo conditions). For the types 1 and 2 copper containing nitrite reductase from *Alcaligenes xylosoxidans*, where we have structures of several mutants as well as the native enzyme, the crystals typically diffract to 1.9 Å at room temperature [25,26] Cryo-annealing has yielded four structures at atomic resolution, including that of the native enzyme which has been determined to 1.04 Å resolution [27]. In fact, these structures represented the first atomic resolution structures of copper proteins. Fig. 1 shows diffraction images from the same crystal before and after cryo-annealing for the native enzyme, demonstrating the dramatic improvement possible from this treatment [24].

Fig. 2 shows how much improvement there is in the quality of electron density maps for data measured between 1.9 and 1.04 Å resolutions, following cryo-annealing. There is also a large increase (six-fold in this example) in the number of independent experimental observations (data points) as the resolution increases. This further advances the level of structural detail that can be modelled reliably, so that, as well as improved accuracy and precision of metrical data, anisotropic thermal motions, positions of H atoms and multiple conformations of amino acid residues can be seen. Atomic resolution may also reveal other features of the structure not visible at lower resolution, e.g. flexible regions or chain termini. These are all illustrated in Figs. 3–5 using the structure of *A. xylosoxidans* Cu nitrite reductase. Overall, the atomic resolution structures of the native protein and its D92E mutant (at 1.12 Å) have led to a deeper understanding of the structural features and the catalytic mechanism of this enzyme. The major regions of disorder in the structure, the identity of the substrate entry pocket, clarification of the structure of the water network leading from the protein surface to the catalytic copper, disorder of specific residues at the type 2 copper centre that imply a role in catalysis—all these aspects of the crystal structure and

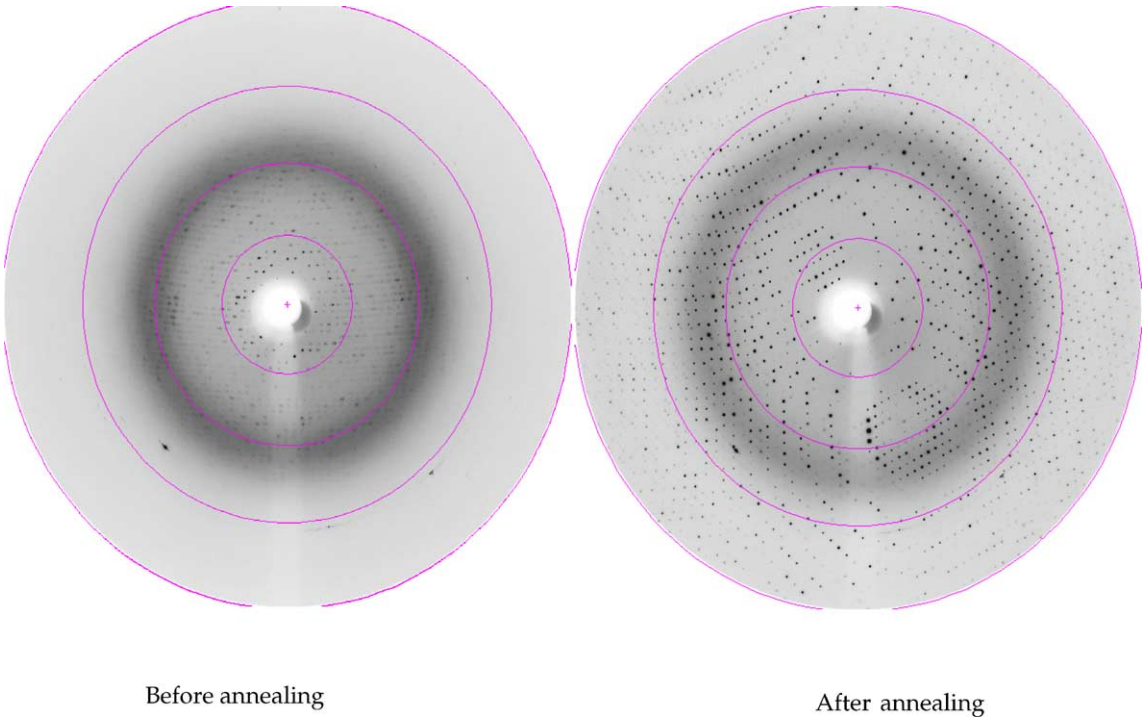

Fig. 1. The benefit of using in-situ cryogenic annealing to improve the quality of diffraction by flash frozen protein crystals is illustrated by diffraction images from the same crystal of *A. xylosoxidans* Cu nitrite reductase. Resolution rings are shown at 8.2, 4.1, 2.7 and 2.0 Å. Before annealing the diffraction limit is 2.5 Å. Following cryo-annealing, the diffraction extends to 1.04 Å, well beyond the 2 Å limit of the displayed image. This figure is reprinted from reference [24] by permission of IUCr.

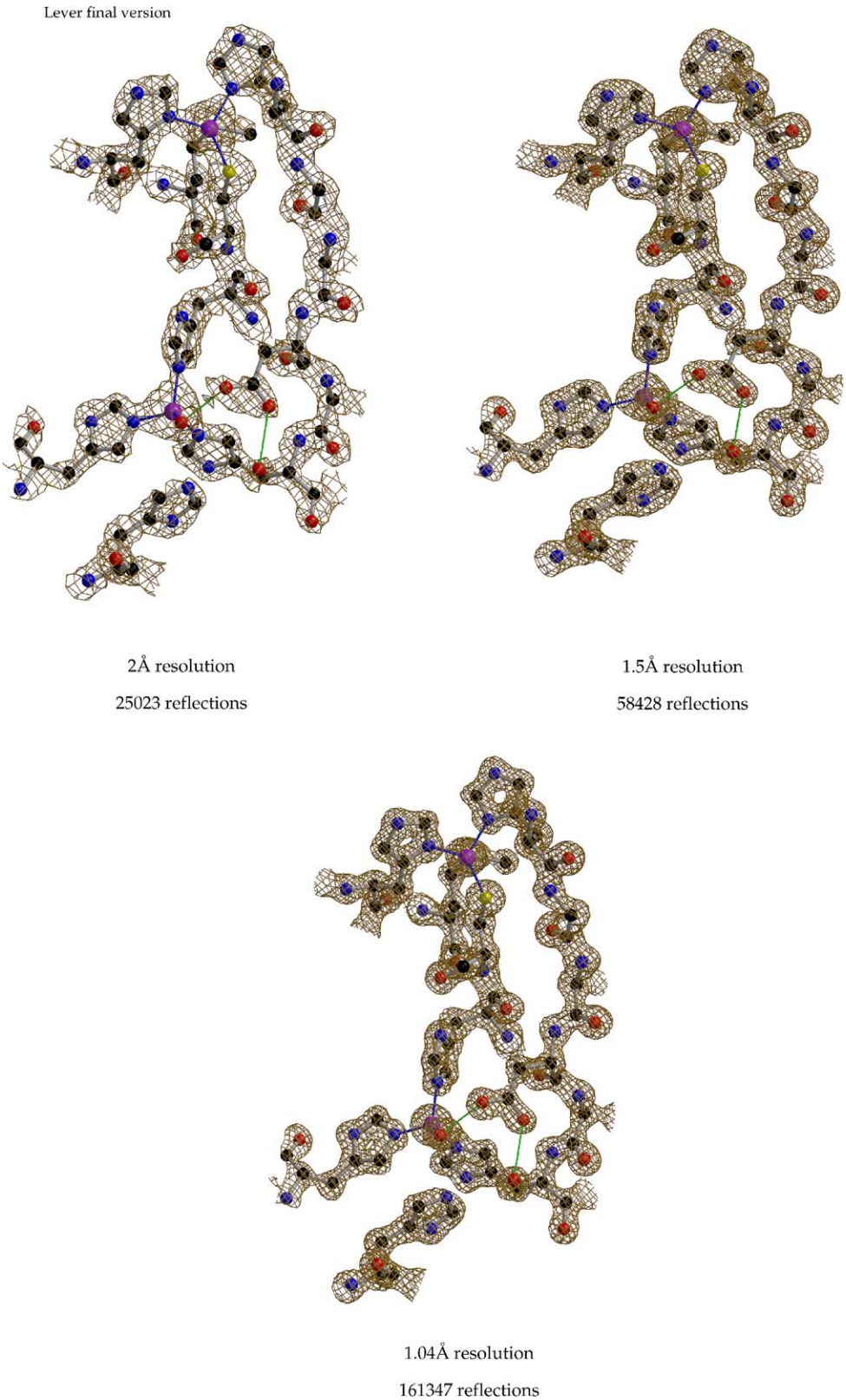

Fig. 2. Electron density maps taken at three resolutions taken from independent crystal structures of *A. xylosoxidans* nitrite reductase, to illustrate the increased observation content and the enhancement of map quality that follows from increasing the diffraction limit.

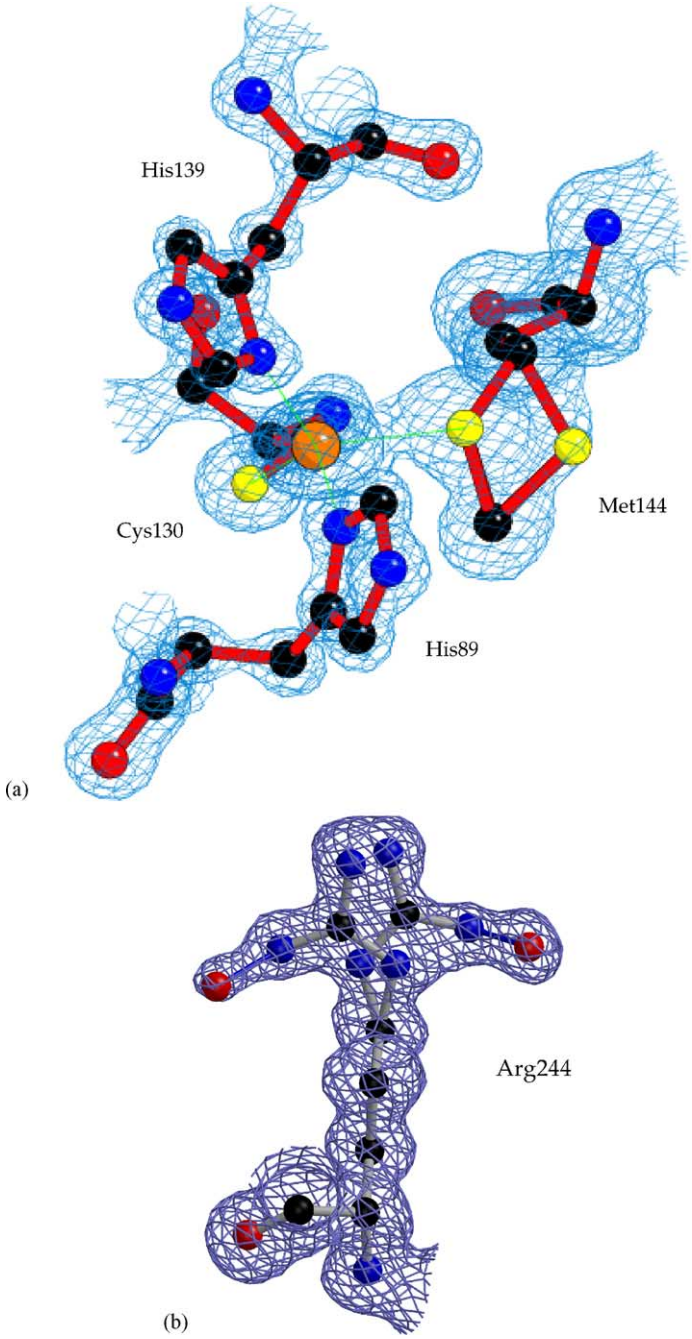

Fig. 3. Electron density maps illustrating multiple orientations of amino acid sidechains in the 1.04 Å resolution *A. xylosoxidans* nitrite reductase structure. (a) The Met144 ligand at the type 1 copper site adopts a dual conformation in which the S atom is positioned at 2.45 Å and 4.25 Å from the Cu with 90:10 occupancy respectively; (b) a 50:50 dual conformation for the Arg244 residue. These features of the structure are not revealed at lower resolutions.

their biological significance have been revealed by atomic resolution data [27]. They are hidden or obscured at lower resolutions. In this context, we would like to note that the size of crystals used for both the native enzyme and D92E mutant was about 0.1 mm × 0.1 mm × 0.4 mm, at least an order of magnitude smaller than what is required for neutron crystallography, which has a major strength in defining the position of hydrogen atoms (Fig. 6).

Another method of improving the diffraction quality of protein crystals involves reversible hydration and dehydration of the crystal in situ [28]. This method was used to optimise the synchrotron based diffraction of carbon monoxide dehydrogenase, improving the resolution range from 2.2 to 1.1 Å [9].

Another community to benefit from increased accuracy is the quantum chemist who, with the rapid advances in computer technology, is looking to tackle larger systems at the electronic level (e.g. [29]). We have witnessed tremendous increases in computational speed and efficiency in recent years, a trend that shows every sign of continuing, at least

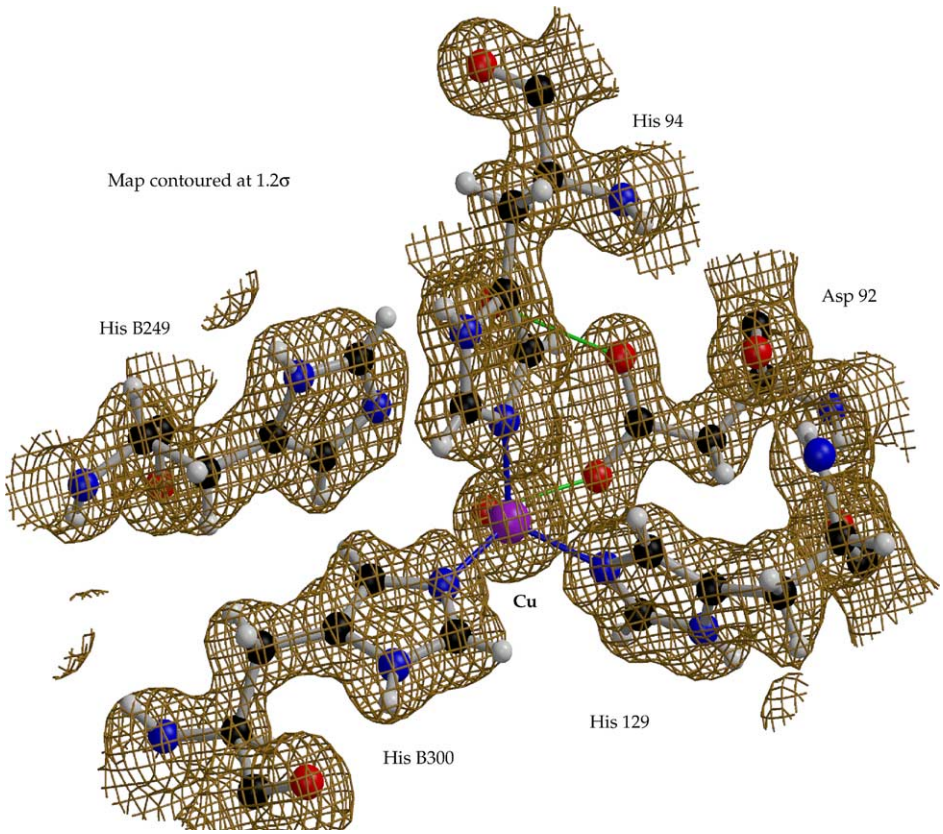

Fig. 4. Several hydrogen atoms can be placed in the electron density map at 1.04 Å resolution. H-atoms make their strongest contribution to the diffraction data at low resolutions and are often included as 'riding hydrogens' during crystallographic refinement. However, they but can only be accurately modelled ('seen' and placed in the electron density) at atomic or higher resolution. Accurate and precise modelling of H-atoms in a structure are important factors in understanding the catalytic processes in metalloproteins and their dynamic properties.

in the in the near future. This means that theoretical calculations that were previously computationally prohibitive are now becoming feasible, especially when using fast parallel processing algorithms. For example, quantum mechanical modelling of metal centres involved in substrate binding and activation or in electron transfer reactions are now realistic targets. High quality, atomic resolution input data are essential for a successful outcome of such an approach. In particular, accurate and precise positioning of hydrogen atoms and water molecules are necessary and this is only achievable at atomic or better (i.e. <1 Å) resolution.

5. 3D-EXAFS and medium resolution crystallography: improvement to atomic resolution accuracy

In principle XAFS is capable of providing important metrical data on any metal-containing protein or other biological molecules. Historically, the majority of applications have used spherically averaged frozen solution measurements to extract this data, which usually consists of a set of one-dimensional metal-scattering atom distances and their associated Debye–Waller terms. Changes in these parameters and/or the scattering atom coordination numbers when the metal centre is perturbed (e.g. by catalysis) give the desired structural information, which can then quite often be related to the biological function of the system under study. In some cases the types of nearest neighbour atoms to the metal and the first (inner) shell metal-scattering atom distances may provide sufficient detail. In other cases it is often necessary to include many shells and many multiple scattering (MS) paths to adequately simulate an EXAFS spectrum. The nature of MS and how it may be exploited to yield important structural information have been the subjects of many papers (e.g. [30–33]; also, see the paper by Lay & Armstrong in this volume). As geometric content is inherent in EXAFS data containing MS, simulations using MS theory enable the extraction of two or even three-dimensional structural features of the metal coordination. A proper picture of these MS processes occurs when a simulation accounts for high order, many atom scattering paths using exact curved wave theory, and where a complete set of inter- as well as intra-ligand scattering events are included. This leads on to the idea of 3D-EXAFS [3], where existing three-dimensional structures of metalloproteins, available in the PDB, can be used in combination with EXAFS data, to give the most detailed view possible of the metal centres that form the core of this important class of protein.

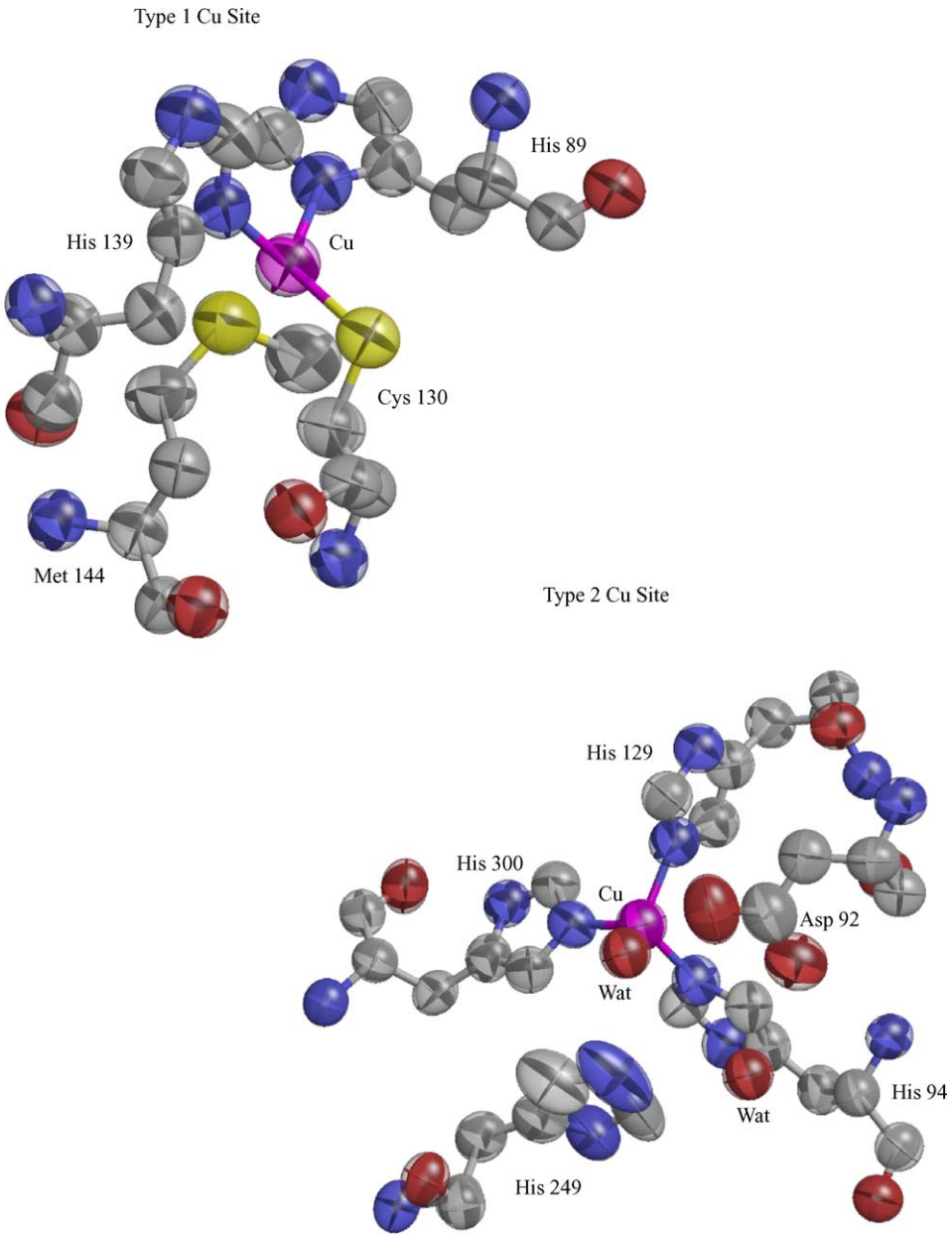

Fig. 5. Thermal ellipsoids shown at the 50% probability level for the type 1 and type 2 Cu environments of *A. xylosoxidans* nitrite reductase, calculated using the 1.04 Å resolution crystal structure [27]. These data show the overall stability of the two environments whilst also highlighting the more dynamic/flexible components: at the type 2 Cu, the Asp 92 and His 249 residues show much greater anisotropy than the three ligating histidine residues, a result that provides structural evidence in favour of their probable role in substrate binding and utilisation. At the type 1 Cu most anisotropy is observed in the metal ligands Met144 and His 139. The latter is exposed to the surface of the protein and has a probable role in electron transfer from the donor protein. The Met144 is a weak ligand to the Cu atom and actually adopts two different positions in the crystal structure (See Fig. 3). Atomic resolution is required to observe these kind of anisotropic features in a crystal structure. These figures were generated using *Rastep* [38].

A typical application of the this approach occurs when crystallographic information is available for some state of a metalloprotein but not for others; for example, the resting state structure may be known but crystallographic data on reactive intermediates may be lacking. In such circumstances EXAFS data on different states of the protein may be solved by the combined approach to predict structural features of these intermediates. Similar considerations apply when studying the effect of mutations that may influence the function or structure of the metal centre.

The advantages of 3D-EXAFS over 'conventional' single shell or 'shell by shell' or 'model ligand' methods of EXAFS analysis are:

- known and relevant protein structures are used as starting data;

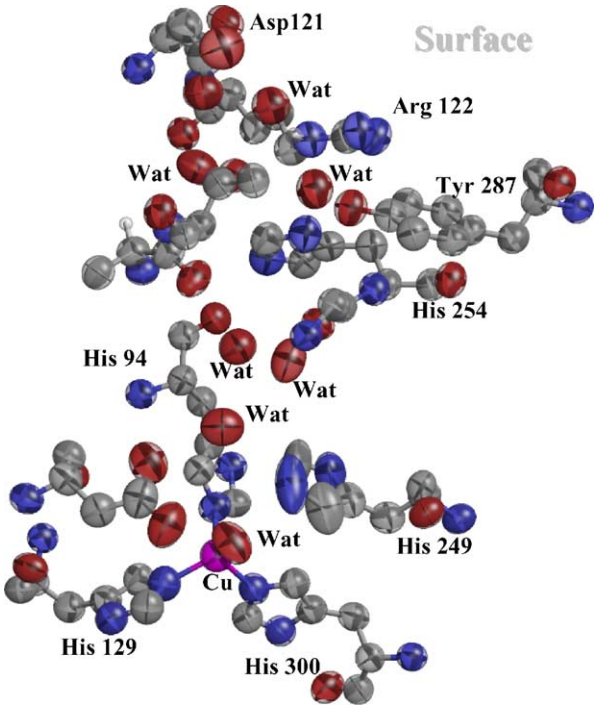

Fig. 6. The active site proton channel in *A. xylosoxidans* nitrite reductase. The positions of water molecules in the channel are well defined and their associated thermal ellipsoids are elongated in the overall direction of the proposed electron flow from the surface.

- crystallographic restraints on geometry (and internal distances of atoms in a given residue, e.g. atoms within an imidazole ring) can be applied;
- chemically and physically realistic results are guaranteed;
- EXAFS results are directly comparable to the input PX data;
- EXAFS output may be used as restraints in the final phase of crystallographic analysis of the metal centre when the resolution of the crystallographic structure is not close to atomic;
- EXAFS information is resolution independent and can provide a sub-atomic resolution picture of the metal centre from PX input data of any resolution. This is particularly significant given that the majority of metalloprotein crystal structures to date are between 1.5 and 2 Å resolution; and
- in the future, single crystal XAFS and PX experiments can be combined and the polarised nature of the X-rays from SR exploited to pick out specific features of the metal binding environment (e.g. in catalytically active crystals). Time resolved 'movies' of the metal site in crystals may be possible using this combination.

While future efforts in crystallography might usefully be directed towards obtaining increasing numbers of atomic resolution structures, the majority are likely to be at high resolution or lower (∼1.5–3.0 Å). This is the probable outcome of several high-throughput PX projects where the objective is to acquire hundreds (or even thousands) of crystal structures each year. In this connection, 3D-XAFS has a potentially important role in refining the stereochemistry at the metal centre. Two examples illustrate this role. First, consider Fig. 7, which shows 3D-EXAFS simulations of solution EXAFS data for the type 2 Cu centre of *A. xylosoxidans* nitrite reductase, using crystal structures measured and refined at three different resolutions: 3 Å [1ndr.pdb] [34], 1.9 Å [1hau.pdb] [26] and 1.04 Å [1oe1.pdb] [27]. In each simulation the crystal structure coordinates are used directly (without refinement) to calculate the theoretical fits [33]. The curve calculated using the 1.04 Å resolution data is in excellent agreement (fit index 0.65) with the experimental spectrum and is clearly superior to the simulations obtained using the coordinates of the medium (fit index 5.4) and low resolution (fit index 6.3) structures. Inspection of Table 4 provides the explanation for this: the water molecule is placed at 1.7 Å from the type 2 Cu in both of the lower resolution structures whereas it is at the chemically more reasonable distance of 1.95 Å in the atomic resolution structure, while the three histidine ligands are shorter by ∼0.1 Å. A 3D-EXAFS refinement, starting with the 3 Å resolution coordinates leads to the same shifts in the positions of the ligands as observed in going from 3 to 1.04 Å crystallographic structure, and gives good agreement ('converges') with the atomic resolution crystal data.

In the second example, 3D-EXAFS was used to enhance the information content of the FeMo-cofactor obtained by the crystallographic refinement of MoFe *K. pneumoniae* nitrogenase at 1.6 Å resolution [35]. A substantial agreement between the XAFS and PX metrical data for the heavier Fe and S atoms was observed (Table 5) [36], while the main differences were seen in the positions of the lighter histidine and homocitrate ligands. The N(His) moved by ∼0.2 Å while the homocitrate O moved by ∼0.15 Å in the 3D-EXAFS refinement. These results were then used as restraints in further cycles of 1.6 Å crystallographic refinement, which led to a better agreement between the two techniques. Rees and co-workers subsequently determined the structure of *A. vinelandii* nitrogenase at 1.16 Å [11] and comparison with their crystallographic coordinates shows little difference

Table 4
Bond lengths at the type 2 Cu centre of *A. xylosoxidans* nitrite reductase determined from three independent crystal structures at resolutions of 3, 1.9 and 1.04 Å

	Crystal structure resolution		
	3.0 Å	1.9 Å	1.04 Å
Bond length (Å)			
Cu–His 94	2.08	2.02	1.96
Cu–His 129	2.09	2.04	1.99
Cu–His 300	1.96	2.26	1.90
Cu–Water	1.70	1.71	1.95
Reference	[34]	[26]	[27]

These structures correspond to the 3D-EXAFS simulations shown in Fig. 7.

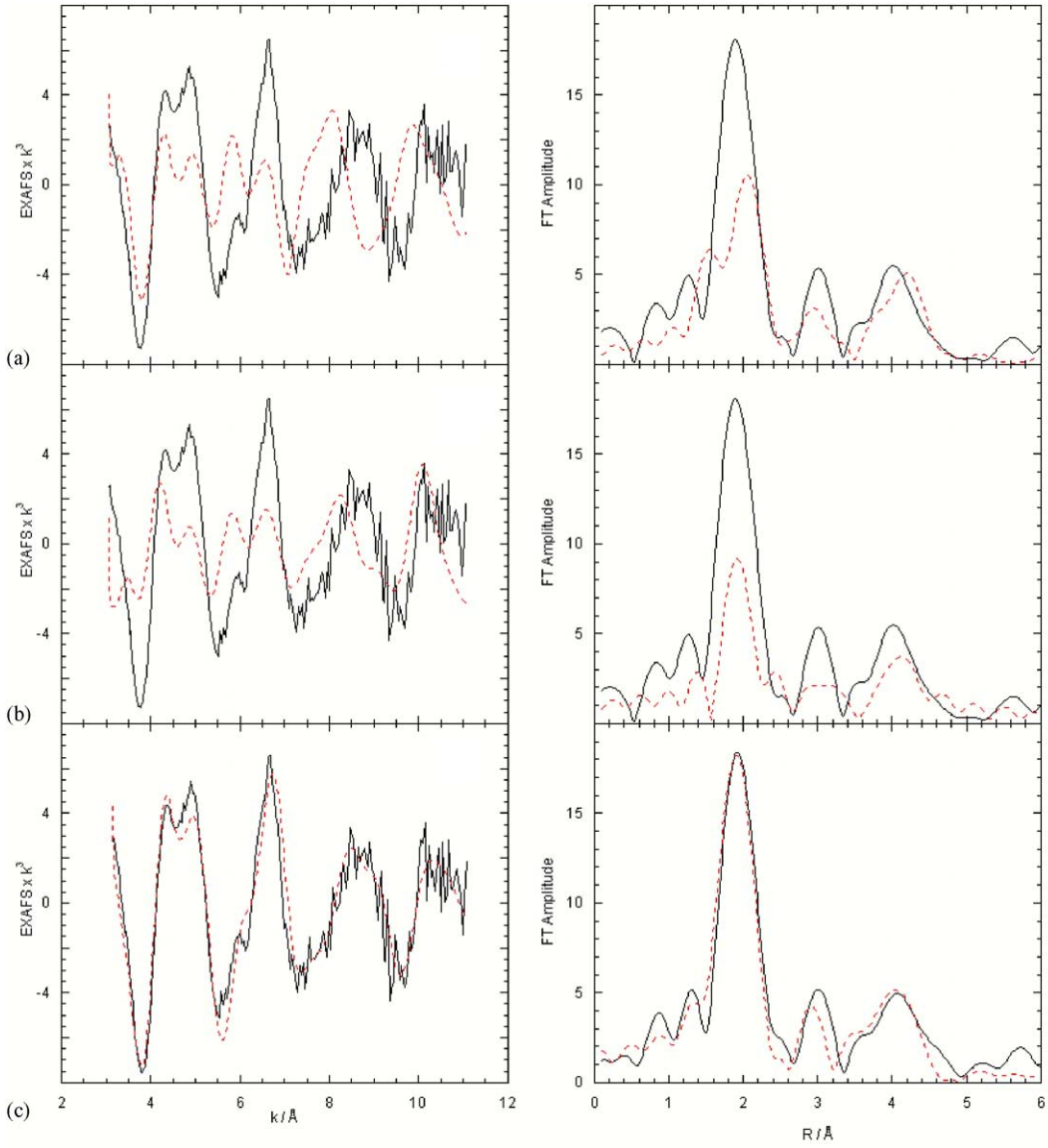

Fig. 7. The k^3-weighted K-edge X-ray absorption spectrum of the type 2 Cu site of *A. xylosoxidans* nitrite reductase and 3D-EXAFS simulations (dashed lines), calculated using three independent crystal structures at (a) 3.0 Å [34]; (b) 1.9 Å [26]; and (c) 1.04 Å [27] resolutions. This figure is reprinted from [33] by permission of IUCr.

between the EXAFS-restrained 1.6 Å *K. pneumoniae* structure and the 1.16 Å atomic resolution structure.

These examples show that accurate metal–ligand information, normally only available by crystallography at atomic resolution, can be obtained by 3D-EXAFS refinements using crystal structure data at lower resolution as starting parameters. The case of nitrogenase also shows how the output of a 3D-EXAFS analysis may be used to advantage as additional restraints during crystallographic refinement.

Among the several opportunities for combining medium to low resolution PX data with XAFS are time resolved studies aimed at examining reaction intermediates. The existence of rapid scanning monochromators for recording 'quick exafs' (QEXAFS) spectra means that biochemical processes on the milliseconds (for XANES) to seconds (for EXAFS) time scales are now accessible using XAFS. Alternatively, stopped-flow or rapid freeze quench methods can be used to trap kinetic reaction intermediates. These experiments can be performed at increasingly lower protein concentrations due to technological improvements in high count rate, high resolution solid state X-ray fluorescence detectors and in the use of high brightness, focussed beamlines at synchrotrons. 'Steady-state' crystallographic data can be taken as the starting model for 3D-EXAFS refinement of the 'frozen' reaction intermediate data.

6. Conclusions and future directions

It is clear that metalloproteins, in exploiting the redox properties of the metal centre, trigger a chemical reaction

Table 5
3D-EXAFS of the Mo K-edge of *Klebsiella pneumoniae* nitrogenase

Ligand	1.6 Å resolution				1.16 Å resolution	
	First refinement		Second refinement		ΔR (Å)	Crystal values (Å)
	R (Å)	σ^2 (Å^2)	R (Å)	σ^2 (Å^2)		
Mo–N(His)	2.48	0.11	2.29	0.003	−0.17	2.29
Mo–O5 (homoct)	2.29	0.11	2.14	0.001	−0.16	2.18
Mo–O7 (homoct)	2.35	0.11	2.31	0.001	−0.04	2.20
Mo–S1B	2.30	0.001	2.30	0.001	0.0	2.33
Mo–S3B	2.38	0.001	2.37	0.001	−0.01	2.37
Mo–S4B	2.35	0.001	2.35	0.001	0.00	2.33
Mo–Fe7	2.67	0.006	2.67	0.006	0.00	2.67
Mo–Fe6	2.68	0.006	2.67	0.006	−0.01	2.67
Mo–Fe5	2.71	0.006	2.71	0.006	0.00	2.67
Mo–Fe2	5.04	0.01	5.04	0.01	0.00	5.04
Mo–Fe3	5.06	0.01	5.06	0.01	0.00	5.05
Mo–Fe4	5.09	0.01	5.08	0.01	−0.01	5.10

In the first refinement distances were fixed at the 1.6 Å resolution crystal structure [35] values while the Debye–Waller (σ^2) values were refined; in the second refinement the distances were also refined. A higher value of σ^2 than 0.03 Å^2 signifies that an atom is incorrectly placed and that little contribution to XAFS signal is made. ΔR is the difference in Mo–ligand distance from the crystallographic value averaged over the two independent αβ units of the protein. The final column includes data from the 1.16 Å resolution crystal structure of *A. vinellandii* [11].

through only small changes at the metal site, thus requiring very high accuracy in structure determination to pinpoint these changes. Such accuracy can be provided by the crystal structures at atomic resolution, defined as 1.2 Å or less. At such resolution, not only are the positions of individual atoms sufficiently accurately defined but also their anisotropic behaviour is also reasonably well defined. With improvements in crystallisation techniques, as well as in the SR technology including source and detectors, more and more structures are likely to be determined at these resolution. In this context, the technique of in situ 'cryo-annealing' holds significant promise. It is likely that by using small well formed crystals, crystal quality could be further improved by cryo-annealing, presumably by reducing the screw defects in the crystals. The availability of larger numbers of atomic resolution structures would also encourage the development of quantum mechanical calculations which require highly accurate information about the positions of protein atoms but also require the knowledge of associated hydrogen atoms.

As we have noted, currently over 90% of the crystallographic structures are known to >1.5 Å resolution. In these cases, the use of 3D-EXAFS refined coordinates as restraints for the final stage crystallographic refinement can be highly advantageous. With the increased availability of single crystal XAFS and MAD-PX capability on the same instrument, data complementing each other can be collected from the same crystal. In this case, effort is required for the rigorous analysis methods for XANES calculations and refinement approaches.

References

[1] W.E.B. Shepard, B.F. Anderson, D.A. Lewandoski, G.E. Norris, E.N. Baker, J. Am. Chem. Soc. 112 (1990) 7817.
[2] F.E. Dodd, Z.H.L. Abraham, R.R. Eady, S.S. Hasnain, Acta Cryst. D56 (2000) 690.
[3] K.C. Cheung, R.W. Strange, S.S. Hasnain, Acta Cryst. D D56 (2000) 697.
[4] S. Yoshikawa, K. Shinzawa-Itoh, T. Tsukihara, J. Inorg. Biochem. 82 (2000) 1.
[5] H. Schindelin, C. Kisker, D.C. Rees, JBIC 2 (1997).
[6] A. Messerschmidt, R. Huber, T. Poulos, K. Weighardt, in: Handbook of Metalloproteins, 2001.
[7] G.M. Sheldrick, T.R. Schneider, in: SHELX: High-Resolution Refinement, 1997.
[8] A. Abola, F.C. Bernstein, S.H. Bryant, T.F. Koetzle, J. Weng, in: F.H. Allen, G. Bergerhoff, R. Sievers (Eds.), Protein Data Bank, Bonn, 1987.
[9] H. Dobbek, L. Gremer, R. Kiefersauer, R. Huber, O. Meyer, Proc. Natl. Acad. Sci. U.S.A. 99 (2002) 15971.
[10] M. Gnida, R. Ferner, L. Gremer, O. Meyer, W. Meyer-Klauke, Biochemistry 42 (2003) 222.
[11] O. Einsle, F.A. Tezcan, S.L.A. Andrade, B. Schmid, M. Yoshida, J.B. Howard, D.C. Rees, Science 297 (2002) 1696.
[12] J.M. Guss, H.D. Bartunik, H.C. Freeman, Acta Cryst. B 48 (1992) 790.
[13] R. Durley, L. Chen, L.W. Lim, F. Scott Mathews, V.L. Davidson, Protein Sci. 2 (1993) 739.
[14] L.M. Cunane, Z.W. Chen, R.C.E. Durley, F.S. Mathews, Acta Cryst. D 52 (1996) 676.
[15] A. Romero, H. Nar, R. Huber, A. Messerschmidt, A. Kalverda, G.W. Canters, R. Durley, F. Scott Mathews, J. Mol. Biol. 236 (1994) 1196.
[16] H. Nar, A. Messerschmidt, R. Huber, M. van de Kamp, G.W. Canters, J. Mol. Biol. 221 (1991) 765.
[17] E.N. Baker, J. Mol. Biol. 203 (1988) 1071.
[18] L.M. Murphy, S.S. Hasnain, R.W. Strange, I. Harvey, W.J. Ingledew, in: S.S. Hasnain (Ed.), XAFS Studies on the Blue Copper Proteins: the Effect of pH and Oxidation State Changes on the Copper Site, Chichester, 1991.
[19] A. Lommen, K.I. Pandya, D.C. Koningsberger, G.W. Canters, Biochim. Biophys. Acta 1076 (1991) 439.
[20] L.M. Murphy, R.W. Strange, G. Karlsson, L. Lundberg, T. Pascher, B. Reinhammar, S.S. Hasnain, Biochemistry 32 (1993) 1965.
[21] Z. Dauter, V.S. Lamzin, K.S. Wilson, Curr. Opin. Struct. Biol. 7 (1997) 681.
[22] C.E.M. Stevenson, S.M. Mayer, L. Delarbre, D.M. Lawson, J. Cryst. Growth 232 (2001) 629.
[23] S. Kriminski, C.L. Caylor, M.C. Nonato, K.D. Finkelstein, R.E. Thorne, Acta Cryst. D 58 (2002) 459.
[24] M.J. Ellis, S. Antonyuk, S.S. Hasnain, Acta Cryst. D 58 (2002) 456.
[25] F.E. Dodd, J. Van Beeumen, R.R. Eady, S.S. Hasnain, J. Mol. Biol. 282 (1998) 369.
[26] M.J. Ellis, F.E. Dodd, R.W. Strange, M. Prudêncio, G. Sawers, R.R. Eady, S.S. Hasnain, Acta Cryst. D 57 (2001) 1110.
[27] M.J. Ellis, F.E. Dodd, G. Sawers, R.R. Eady, S.S. Hasnain, J. Mol. Biol. 328 (2003) 429.
[28] R. Kiefersauer, M.E. Than, H. Dobbek, L. Gremer, M. Melero, S. Strobl, J.M. Dias, T. Soulimanee, R. Huber, J. Appl. Cryst. 33 (2000) 1223.
[29] U. Ryde, K. Nilsson, J. Am. Chem. Soc. 125 (2003) 14232.
[30] R.W. Strange, N.J. Blackburn, P.F. Knowles, S.S. Hasnain, J. Am. Chem. Soc. 109 (1987) 7157.
[31] N. Binsted, R.W. Strange, S.S. Hasnain, Biochemistry 31 (1992) 12117.
[32] S.S. Hasnain, K.O. Hodgson, J. Synchrotron Rad. 6 (1999) 864.

[33] S.S. Hasnain, R.W. Strange, J. Synchrotron Rad. 10 (2003) 9 (and other articles in this issue).
[34] F.E. Dodd, S.S. Hasnain, Z.H.L. Abraham, R.R. Eady, B.E. Smith, Acta Cryst. D 53 (1997) 406.
[35] S.M. Mayer, D.M. Lawson, C.A. Gormal, S.M. Roe, B.E. Smith, J. Mol. Biol. 292 (1999) 871.
[36] R.W. Strange, R.R. Eady, D. Lawson, S.S. Hasnain, J. Synchrotron Rad. 10 (2003) 71.
[37] R.A. Engh, R. Huber, Acta Cryst. A47 (1991) 392.
[38] E.A. Merritt, D.J. Bacon, Methods Enzymol. 277 (1997) 505.